Multi-Agent Based Optimal Scheduling and Trading for Multi-Microgrids Integrated with a Transportation Network

Yun Liu, *Member, IEEE,* Hoay Beng Gooi, *Senior Member, IEEE,* Yuanzheng Li, and Huanhai Xin, *Member, IEEE,*

***Abstract*—This paper investigates multi-period optimal energy scheduling and trading for multi-microgrids (MMGs) integrated with a transportation network. Specifically, an optimization based multi-period traffic assignment model is built to characterize the vehicular flows considering elastic travel demands and rational drivers. Meanwhile, each microgrid (MG) is modeled to independently schedule its operation via MG energy trading and providing electric vehicle (EV) charging service with its fast charging stations (FCSs). The EV charging prices could further influence traffic flow distribution of the transportation network. To co-optimize the coupled system, a multi-agent based optimal scheduling and trading (MABOST) scheme is proposed, which is facilitated by peer-to-peer communication of trading quantities and prices among the agents, thus can preserve privacy of the market participants. Within the scheme, the MGs and EVs take their optimal decisions in response to MG energy trading and EV charging prices updated via bilateral negotiation based on the demand-supply relationship. When an equilibrium of the coupled system is reached, each MG can minimize its operation cost, and the traffic condition could also be improved. A case study of a 4-MG system coupled with a double-ring transportation network is conducted to validate effectiveness of the scheme.**

***Index Terms*—Electric vehicle charging, energy management and trading, multi-agent system, multi-microgrids, transportation network.**

I. Introduction

Microgrids (MGs) are envisaged as the basic building blocks of the future active distribution system [1]. Facilitated by the advanced metering, communication, and control technologies, these MGs can be organized in a decentralized structure, which enjoys the merits of more flexible grid configuration and reliable energy supply [2]. Moreover, in the forthcoming deregulated power market, each MG operator functions as an independent market participant in the peer-to-peer energy and reserve market to substantially maximize its benefit via energy trading/sharing [3], [4].

Different from the conventional centralized decision making, each functional entity (i.e. MG in this context) distributively optimizes its sub-objective with respect to its own local variables [5]. Within this decentralized architecture, extensive research has been conducted to achieve distributed optimal energy scheduling/trading within the multi-microgrids (MMGs). To name a few, Gregoratti and Matamoros proposed a single-period distributed energy trading scheme among the MMGs based on the dual decomposition algorithm [6]. Wang and Huang further modeled the participation of responsive loads and proposed a multi-period energy trading and scheduling strategy for the MMGs based on Nash Bargaining Game [7]. Considering that various uncertain factors (e.g. load demand and renewable power generation) exist in the operation of the MMGs, a stochastic optimization based hierarchical bi-level control scheme is proposed for distributed decision making of the MMGs [8]. In [9], an online ADMM with regret was applied to solve a similar problem.

In recent year, electric vehicles (EVs) are proliferating due to their eco-friendliness and policy support from governments. However, as the proportion of EVs keeps increasing, the charging activities depending on the traffic conditions can severely change the load demand pattern, which may endanger the grid operation concerning the adequacy of the grid capacity, especially when they synchronize with the system peak demand [10]. To alleviate this negative effect and motivated by the strong coupling between the MMGs and EVs, Wang *et al.* designed an integrated energy exchange scheduling for MMGs and EVs with the objectives to bring down MG electricity costs as well as avoid frequent switch between battery charging/discharging states [11]. Zou *et al.* proposed a decentralized gradient projection method utilizing EVs to reduce the variation of the total demand trajectory while maintaining a satisfactory operation cost of the MMGs [12].

References [11], [12] both utilize demand response of EV batteries to enhance the optimality of the power distribution side. However, consider that public fast charging station (FCS) may remain the major energy sources for EVs in cities with low home charging penetration (e.g., Beijing and Shanghai of China) [13], different FCS pricing schemes could influence of traffic conditions on EV routing, which in turn redistribute the EV charging demand. Currently, it is a major research trend to investigate the coupling effect of the transportation and power distribution systems to simultaneously improve their performances. To this end, Wei *et al.* characterized the steady-state traffic flow pattern using the Wardrop user equilibrium (UE) and designed a robust operation of distribution networks considering the impact of road congestion on routing decision [14]. Alizadeh *et al.* studied the optimal pricing scheme to coordinately optimize operation of the power and transportation networks. Specifically, a congestion-sensitive plug-in fee is enforced to guide the user-equilibrium vehicular flows to the social optimum [15]. Following a similar philosophy, Wei *et al.* studied the network equilibrium of coupled transportation and power distribution system using a locational marginal pricing scheme. This scheme can indirectly suppress traffic congestion as it requires a higher price if the charging demand is extremely high in a certain FCS [16]. However, these works only exploit the synergies of electrical and transportation networks from the spatial perspective.

In this paper, the spatial-temporal interaction of the emerging MMGs and the transportation network is investigated. Within the considered framework, each MG can be regarded as an integrated energy service provider (IESP) serving electric loads of a certain region. With the objective to maximize its profit, each IESP may equip its MG with cheap generation

units (e.g., renewable energy) and invest a few FCSs to provide EV charging services induced by the prosperity of EV industry. Considering that the MG IESPs, the transportation operator and the main grid operator and can be regarded as independent functional/coperate agents, they are not willing to share their key operational information with others and mainly concerned with their own profits. In light of this, a multi-agent based optimal scheduling and trading (MABOST) scheme is proposed for the coordination of the MMGs and the transportation network. This scheme allows each agent to independently determine its own operational schedule based on peer-to-peer communication of transactive energy [17] information within the multi-agent framework.

The main contributions of this work are twofold. Firstly, a comprehensive model of the MMGs integrated with FCSs is formulated which differs from existing works in three ways: i) it extends the analysis to a multi-period traffic assignment (MPTA) problem [18], and builds a convex optimization model to characterize its UE considering that the drivers all behave rationally and are flexible in their travel time; ii) The proposed model not only considers interaction between the electrical and transportation networks, but also that among different regional IESPs, which is consistent to the organizational structure of the future smart grid; iii) A simple yet practical function is derived to approximate the FCS flow-time relationship based on the $M/M/c/K$ queuing theory [19] which is different from that adopted in [16]. Secondly, this work proposes a privacy-preserving MABOST scheme where different market participants interact with each other via price negotiations and take their best responses. Transforming this scheme to an ADMM algorithm solving a constructed convex optimization problem guarantees that a market equilibrium can be iteratively reached, where the operational costs of the MGs can be reduced while the traffic conditions can be improved by alleviating rush-hour traffic and uneven utilization of the FCSs.

The rest of this paper is organized as follows: Section II models to operation of MMGs integrated with a transportation network and formulates the problem to be solved. In Section III, the MABOST scheme is developed, and its economic implication and convergence property are discussed. Numerical results and conclusions are presented in Sections IV and V, respectively.

The major notations of sets, parameters, and variables are listed in Table I. Any variable with superscript t denotes its value at time slot t, while any variable in bold font denotes its corresponding column vector for $t \in \mathcal{T} \triangleq \{1, \cdots, T\}$, where $\mathcal{T}$ is the set of time intervals consisting of the scheduling horizon. Specifically, **0**/**1** denotes an all-zero/one vector. $\intercal$ denotes the transpose of the corresponding vector. Any variable with k in a parentheses to its right (e.g. $\boldsymbol{x}(k)$) denotes its value in the kth iteration. A variable in a calligraphic font (e.g. $\mathcal{S}$) denotes a set, and $|\mathcal{S}|$ is used to denote its cardinality. A capital letter denotes a matrix, and $[\cdot]_{ij}$ indicates the (i,j)th entry of the corresponding matrix.

II. Problem Formulation

This section introduces the mathematical models of MPTA and operation of the MMGs, respectively, and concludes with the problem to be solved.

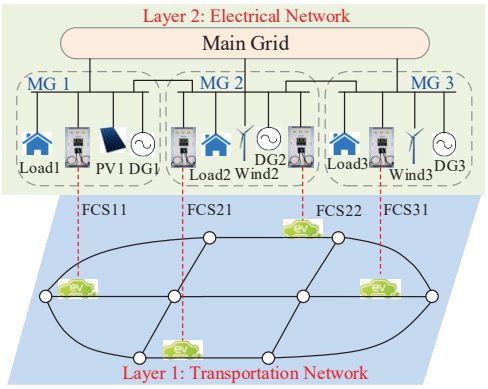

Fig. 1. Illustration of coupling between the MMGs electrical network and transportation network.

TABLE I
Notations of Major Sets, Parameters and Variables

Transportation Network:	
v	Type of vehicles being e or g for EV and GV
rs	index of O-D pair from node r to s
$\mathcal{T}/T$	Index set/total number of time slots
$\mathcal{V}_T/\mathcal{D}_T$	Index set of nodes/O-D pairs
$\mathcal{E}_T$	Index set of links
$\mathcal{E}_u$	Index set of road/FCS/bypass links (u=RD/FCS/BY)
$N_{v,rs}$	Number of feasible routes for type v from r to s
$\Delta_{v,rs}$	Matrix defining the routes of type v from r to s
$\check{\boldsymbol{d}}_{v,rs}$	Quantity of type v intending to travel from r to s
$D_{v,rs}$	Matrix of redistribution of type v from r to s
$F_{v,rs,i}$	Matrix of redistribution of type v on route i of (r,s)
$\boldsymbol{f}_a$	Vehicular flow rate on link $a \in \mathcal{E}_T$
$t_a(\cdot)$	The time a vehicle spending on link $a \in \mathcal{E}_T$
t_{a0}/c_a	Free travel time/capacity of link $a \in \mathcal{E}_{RD}$
μ	Service rate of a charging pile
$t_{w,a}^{\max}/f_a^{\max}$	Maximum waiting time/vehicular flow of link $a \in \mathcal{E}_{FCS}$
$t_{v,rs,i}^t$	Travel time of type v on route i of (r,s) at time slot t
$c_{v,rs,i}^t$	Travel time cost of type v for route i of (r,s)
$y_{e,rs,i}$	FCS link number of EV route i of (r,s)
ω	Monetary value of travel time
C	Traffic rescheduling cost matrix
E_B	Homogeneous charging energy of an EV
MMG Electrical Network:	
$\mathcal{S}_{MG}$	Index set of the MGs
$\boldsymbol{P}_{Gi}$	Power output of the DG in MG i
$\boldsymbol{P}_{i,0}/\boldsymbol{P}_{i,0}$	Power import/export from/to the main grid
$\boldsymbol{P}_{i,j}$	Power flow from MG j to MG i
$\boldsymbol{P}_{\text{out}i}$	Power MG i selling to adjacent MGs
$\boldsymbol{P}_{FCSij}$	EV charging load at FCS ij
$\boldsymbol{P}_{Li}/\boldsymbol{P}_{REi}$	Ordinary load demand / renewable energy of MG i
pr_s/pr_b	Time-invariant main grid energy selling/buyback price
$\boldsymbol{\lambda}_i$	Energy selling price of MG i
$\boldsymbol{\rho}_a$	EV charging price at FCS link $a \in \mathcal{E}_{FCS}$
y_{FCSij}	FCS link number corresponding to load FCS ij
b_{tran}	Energy transfer cost between MGs
$\mathcal{N}_{FCSi}$	Set of FCSs belonging to MG i
$\mathcal{N}_i$	Set of MGs adjacent to MG i

A. Modeling of the Transportation Network

Extending the models built in [15], [16], this section first introduces the MPTA problem for a transportation network including both gasoline vehicles (GVs) and EVs. On this basis, a convex optimization algorithm is derived to characterize the UE of the MPTA problem. It should be noted that, similar to [16], a non-atomic setting for the vehicular flow is assumed throughout this work (i.e., all the recharged EVs have a homogeneous energy requirement E_B), which is justified from a system-level perspective.

1) Vehicular Flows of the Transportation Network: A transportation network can be represented by a strongly connected digraph $\mathcal{G}_T = (\mathcal{V}_T, \mathcal{E}_T)$, as depicted in Layer 1 of Fig. 1. $\mathcal{V}_T$ denotes the index set of nodes and $\mathcal{E}_T \subseteq \mathcal{V}_T \times \mathcal{V}_T$ denotes the set of links. Specifically, a pair $(i, j) \in \mathcal{E}_T$ indicates that there is a directional link from i to j.

The traffic demand can be described by a set $\mathcal{D}_T \subseteq \mathcal{V}_T \times \mathcal{V}_T$ of origin-destination (O-D) pairs. Specifically, $(r, s) \in \mathcal{D}_T$ implies that there exists vehicles expecting to travel from node r to node s. Vector $\hat{\boldsymbol{d}}_{v,rs} = [\hat{d}^1_{v,rs}, \cdots, \hat{d}^T_{v,rs}]^\intercal$ $(v \in \{g, e\})$ defines the quantity of GVs (EVs) that intends to travel at each time slot for $(r, s) \in \mathcal{D}_T$, which is in p.u. and the base value is selected as 100 vehicles/h. However, in case that the travel expense (which will be modeled in the next subsection) is high in the scheduled travel time t_1, a vehicle may be willing to reschedule its travel time to low-cost time slot t_2. The actual quantity of traffic demand can be defined as a matrix $D_{v,rs} \in \mathbb{R}^{T\times T}$ $(v \in \{g, e\})$, where its (t_1, t_2)th entry denotes the amount of GVs (EVs) that are rescheduled from time slot t_1 to t_2. Therefore, it should be satisfied that

$$D_{v,rs}\mathbf{1} = \hat{\boldsymbol{d}}_{v,rs},\ v \in \{g, e\}. \tag{1}$$

For each O-D pair (r, s), there exists multiple feasible routes, which can be generated off-line as introduced in [16]. These feasible routes can be described with a matrix $\Delta_{v,rs} \in \mathbb{R}^{|\mathcal{E}_T|\times N_{v,rs}}$, where $N_{v,rs}$ is the total number of feasible routes. Each column of the matrix corresponds to a route, whose entry is one if the corresponding link belongs to the route and zero otherwise. Denote $F_{v,rs,i} \in \mathbb{R}^{T\times T}$ as the number of vehicles traveling the ith route of O-D pair (r, s), and its (t_1, t_2)th entry is the number of vehicles being rescheduled from time slot t_1 to t_2 to travel this route. This vehicular flow should satisfy

$$\sum_{i=1}^{N_{v,rs}} F_{v,rs,i} = D_{v,rs},\ v \in \{g, e\}, \tag{2}$$

$$F_{v,rs,i} \geq 0,\ i \in \{1, \cdots, N_{v,rs}\},\ v \in \{g, e\}. \tag{3}$$

A subset of the links $\mathcal{E}_{FCS} \subset \mathcal{E}_T$ can be modeled as FCS links. For each $(i, j) \in \mathcal{E}_{FCS}$, there must also exist $(i, j) \in \mathcal{E}_{BY}$ which indicates that a vehicle can bypass the FCS without charging. The rest of the links belong to the road links, i.e., $\mathcal{E}_{RD} = \mathcal{E}_T - \mathcal{E}_{FCS} - \mathcal{E}_{BY}$. All the EVs traveling in the transportation network are assumed to get charged at exactly one FCS *en route*, while those need no charging can be treated as GVs, i.e., they should not visit any FCS link. For $\forall a \in \mathcal{E}_T$, its link flow equals to the total amount of vehicles traveling through it, which is calculated as

$$\boldsymbol{f}_a = \sum_{v\in\{g,e\}} \sum_{(r,s)\in\mathcal{D}_T} \sum_{i=1}^{N_{v,rs}} [\Delta_{v,rs}]_{ai} F^\intercal_{v,rs,i}\mathbf{1}. \tag{4}$$

2) Travel Expense of Vehicles: Three types of travel costs could be incurred for vehicles traveling in the transportation network:

Equivalent time cost: The travel time at each time slot k on a road link $a \in \mathcal{E}_{RD}$ with a vehicular flow f^k_a can be modeled utilizing the Bureau of Public Roads function as

$$t_a(f^k_a) = t_{a0}\left[1 + 0.15\left(\frac{f^k_a}{c_a}\right)^4\right],\ a \in \mathcal{E}_{RD}. \tag{5}$$

Note that c_a is not a mandatory limit for the vehicular flow, thus it is feasible for $f^k_a > c_a$.

The time that a EV spends in a FCS link can be approximated as

$$t_a(f^k_a) = \frac{1}{\mu} + t^{\max}_{w,a}\left(\frac{f^k_a}{f^{\max}_a}\right)^3,\ f^k_a \leq f^{\max}_a,\ a \in \mathcal{E}_{FCS}, \tag{6}$$

Different from [16] which models the queuing behavior as a single-channel queuing system [20], eq. (6) is formulated based on the *M/M/c/K* queuing model considering that the queuing space in a FCS is not unlimited [19]. $f^{\max}_a$ denotes the maximum allowable flow rate such that the possibility for an EV to be rejected by the FCS does not exceed a certain threshold. A detailed justification of this model can be found in Appendix A of the full version.

The travel time of a bypass link can be ignored, i.e.,

$$t_a(f^k_a) = 0,\ a \in \mathcal{E}_{BY}. \tag{7}$$

The total travel time of a vehicle traveling the ith route of O-D pair (r, s) during time slot k can be calculated as

$$t^k_{v,rs,i} = \sum_{a\in\mathcal{E}_T} [\Delta_{v,rs}]_{ai} t(f^k_a),\ v \in \{e, g\}. \tag{8}$$

Consider $\omega =$ \$10/h as the monetary value of travel time, the equivalent time cost of this route equals to

$$c^k_{v,rs,i} = \omega t^k_{v,rs,i},\ v \in \{e, g\}. \tag{9}$$

Rescheduling cost: Define the rescheduling cost matrix as C, where its (i, j)th entry stands for the value loss when a vehicle intending to travel during time slot i is rescheduled to time slot j. In other words, a vehicle may be willing to change its travel time to another time slot as long as the corresponding travel expense is sufficiently low. From a system-level view, a unified C is considered in this paper without discriminating the vehicle types and travel routes.

Charging cost: In a spatial-temporal charging pricing scheme, each FCS $a \in \mathcal{E}_{FCS}$ adopts a distinct charging price $\boldsymbol{\rho}_a$ which can be determined based on the MABOST scheme introduced in Section III. Define $y_{e,rs,i}$ as the FCS link number of the ith EV route of (r, s). Then, the EV charging cost for the ith route of (r, s) at time slot t is $E_B\rho^t_{y_{e,rs,i}}$.

To sum up, the total expense of a GV/EV rescheduled from t_1 to t_2 to travel the ith route of (r, s) can be calculated as

$$\text{cost}^{t_1t_2}_{g,rs,i} = c^{t_2}_{g,rs,i} + [C]_{t_1t_2}, \tag{10a}$$

$$\text{cost}^{t_1t_2}_{e,rs,i} = c^{t_2}_{e,rs,i} + [C]_{t_1t_2} + E_B\rho^{t_2}_{y_{e,rs,i}}. \tag{10b}$$

3) UE of the MPTA Problem: The main objectives of rational drivers are to autonomously minimize their own travel expenses by selecting proper travel routes and times, which is described by Wardrop's first principle [21]. In this regard, the traffic distribution can spontaneously converge to a UE of the MPTA problem, which is a state that no vehicle can decrease its total travel expense by unilaterally changing its travel route or time [18].

Mathematically, the UE can be characterized as follows. Define the minimum travel expense of a vehicle scheduled to

travel during time slot t_1 from r to s as $u^{t_1}_{v,rs}$ ($v \in \{g,e\}$). Then, the following equations hold:

$$[F_{v,rs,h}]_{t_1t_2} = 0 \Leftrightarrow \text{cost}^{t_1t_2}_{v,rs,h} > u^{t_1}_{v,rs},\ \forall t_2, \tag{11a}$$

$$[F_{v,rs,h}]_{t_1t_2} > 0 \Leftrightarrow \text{cost}^{t_1t_2}_{v,rs,h} = u^{t_1}_{v,rs},\ \forall t_2. \tag{11b}$$

Since it is difficult to directly find the traffic distribution satisfying (11), the following optimization problem is presented:

$$\min\ F_{MPTA}(\boldsymbol{x}_T, [\boldsymbol{\rho}_a]_{a\in\mathcal{E}_{FCS}}) = \sum_{t_1\in\mathcal{T}}\left[\omega\sum_{a\in\mathcal{E}_T}\int_0^{f^{t_1}_a} t_a(\xi)d\xi + \sum_{t_2\in\mathcal{T}}\sum_{v\in\{g,e\}}\sum_{(r,s)\in\mathcal{D}_T}[C]_{t_1t_2}[D_{v,rs}]_{t_1t_2} + \sum_{a\in\mathcal{E}_{FCS}}\rho^{t_1}_a E_B f^{t_1}_a\right] \tag{12}$$

subject to (1)-(4), where $\boldsymbol{x}_T \triangleq \{F_{v,rs,i}|\forall v = \{g,e\}, (r,s) \in \mathcal{D}_T, i \in \mathcal{N}_{v,rs}\}$.

The property of the convex optimization (12) can be summarized as

Proposition 1: The flow pattern that solves (12) is equivalent to the UE of the MPTA problem.

The proof of this equivalency can be acquired by generalizing the analysis in [22], and its details are shown in Appendix B of the full version.

B. Modeling of the MMGs Operation

The MMGs are interconnection of multiple independently-owned MGs (their set is denoted as $\mathcal{S}_{MG}$), which are further connected to the utility grid through distribution lines, as illustrated in Layer 2 of Fig. 1. Each MG is equipped with a dispatchable generator (DG) and renewable energy, and serves the ordinary load and FCS charging load in the corresponding region. Energy storage can be readily included in the formulation, but is not considered for ease of illustration. Note that as this paper considers a time slot of one hour, power and energy may be used interchangeably hereinafter.

The objective of an independently-owned MG $i \in \mathcal{S}_{MG}$ is to minimize its operation cost, which can be mathematically formulated as

$$\min\ \text{cost}_{MGi}(\boldsymbol{x}_i, \boldsymbol{\lambda}_i, [\boldsymbol{\lambda}_j]_{j\in\mathcal{N}_i}, [\boldsymbol{\rho}_{y_{FCSih}}]_{h\in\mathcal{N}_{FCSi}}) \triangleq$$
$$\sum_{t\in\mathcal{T}}\Big\{\overbrace{\text{cost}_{Gi}(P^t_{Gi})}^{\text{i) Generation cost}} - \overbrace{pr_sP^t_{Li}}^{\text{ii) Load revenue}} + \overbrace{pr_sP^t_{i,0} - pr_bP^t_{0,i}}^{\text{iii) Main grid trading cost}} + \underbrace{\sum_{j\in\mathcal{N}_i}[(\lambda^t_j + b_{tran})P^t_{i,j} - \lambda^t_iP^t_{\text{out}i}]}_{\text{iv) MG trading cost}} - \underbrace{\sum_{j\in\mathcal{N}_{FCSi}}\rho^t_{y_{FCSij}}P^t_{FCSij}}_{\text{v) EV charging revenue}}\Big\} \tag{13a}$$

subject to

$$P^{\min}_{Gi} \le P^t_{Gi} \le P^{\max}_{Gi},\ \forall t \in \mathcal{T} \tag{13b}$$

$$0 \le P^t_{0,i}, P^t_{i,0} \le P^{\max}_{i,0},\ 0 \le P^t_{i,j} \le P^{\max}_{i,j},\ \forall j \in \mathcal{N}_i \tag{13c}$$

$$0 \le P^t_{FCSij} \le E_Bf^{\max}_{y_{FCSij}},\ \forall j \in \mathcal{N}_{FCSi} \tag{13d}$$

$$P^t_{Gi} + P^t_{i,0} - P^t_{0,i} + \sum_{j\in\mathcal{N}_i}P^t_{i,j} - P^t_{\text{out}i} + P^t_{REi} = P^t_{Li} + \sum_{j\in\mathcal{N}_{FCSi}}P^t_{FCSij} \tag{13e}$$

where $\boldsymbol{x}_i \triangleq \{\boldsymbol{P}_{Gi}, [\boldsymbol{P}_{FCSih}]_{h\in\mathcal{N}_{FCSi}}, \boldsymbol{P}_{i,0}, \boldsymbol{P}_{0,i}, [\boldsymbol{P}_{i,l}]_{l\in\mathcal{N}_i}, \boldsymbol{P}_{\text{out}i}\}$.

The operation cost of MG i consists of 5 parts as shown in (13a). cost_{Gi} in i) is the generation cost of the DG in MG i during time slot t and can be approximated as

$$\text{cost}_{Gi}(P^t_{Gi}) = a_{Gi}\left(P^t_{Gi}\right)^2 + b_{Gi}P^t_{Gi} + c_{Gi},$$

where a_{Gi}, b_{Gi}, and c_{Gi} denote the cost parameters. The generation cost of renewable energy is ignored. Part ii) is the revenue for serving the ordinary load, and the electricity price to the load is assumed equal to pr_s. As the ordinary load under consideration is non-responsive, this part is a constant and does not affect the optimization. b_{tran} in part iv) accounts for the energy transfer cost, which is exerted on the energy buyer. As there is a one-to-one correspondence between any EV charging load in a certain MG and a FCS link in the transportation network, the subscript y_{FCSij} in v) is used to map the FCSij load to its corresponding link $a \in \mathcal{E}_{FCS}$. Constraints (13b) and (13c) limit the amount of DG power output and power exchange between adjacent MGs. Constraint (13d) specifies the maximum EV charging demand at each FCS due to the limited parking spaces. Equation (13e) is the energy balance constraint within each MG.

To conclude this section, the main problem to be solved is summarized: In the integrated power-transportation networks, each vehicle autonomously minimizes its corresponding travel expense by properly selecting a departure time and a route; while each MG IESP can independently determine its energy trading prices with adjacent MGs and FCS charging prices, as well as optimize its operational schedule. The objective is to find an equilibrium of the coupled system when all the market participants including MG IESPs and vehicles make their optimal decisions.

III. Multi-Agent Based Optimal Scheduling and Trading Scheme

A. Centralized Formulation of the Co-Optimization Problem

To derive the MABOST scheme for MMGs integrated with FCSs, a centralized co-optimization model is first constructed:

$$\min\ F_{Cent} = F_{MPTA} + \sum_{i\in\mathcal{S}_{MG}}\text{cost}_{MGi} \tag{14a}$$

subject to

$$\boldsymbol{x}_T \in \chi_T := \{(1)-(4)\} \tag{14b}$$

$$\boldsymbol{x}_i \in \chi_i := \{(13b)-(13e)\},\ \forall i \in \mathcal{S}_{MG} \tag{14c}$$

$$P^t_{\text{out}i} = \sum_{i\in\mathcal{N}_i}P^t_{j,i},\ \forall i \in \mathcal{S}_{MG} \tag{14d}$$

$$P^t_{FCSij} = E_Bf^t_{y_{FCSij}},\ \forall j \in \mathcal{N}_{FCSi} \tag{14e}$$

The objective function F_{Cent} does not contain much practical significance due to the existence of F_{MPTA} [22]. Constraints (14b) and (14c) are the sets of local constraints specifying the feasible range of $\boldsymbol{x}_T$ and $\boldsymbol{x}_i$. Constraints (14d) creates coupling among the MMGs; while (14e) creates coupling between the FCS charging load and vehicular flow of the corresponding FCS link. Despite the lack of significance of (14a), it is constructed to derive the MABOST scheme. Specifically, It can be observed that (14) is convex and decomposable with respect to $\boldsymbol{x}_T$ and $\boldsymbol{x}_i$ ($i \in \mathcal{S}_{MG}$), thus falls into the canonical form of the ADMM [23]. By transforming the ADMM algorithm following a similar paradigm as in [2] (which is omitted here due to limited space), the following MABOST scheme can be acquired which has a clear economic interpretation in the viewpoints of different agents and is guaranteed to reach an equilibrium of the multi-bilateral energy trading market.

B. Design of the MABOST Scheme

The MABOST scheme is implemented in a multi-agent environment which consists of three types of agents, namely, traffic agent, MG-IESP agent, and main grid agent. In what follows, the algorithm distributively executed at different agents in the kth iteration is to be elaborated.

Traffic Agent: The objective of this agent is to find the most economic-efficient route and travel time for each vehicle following the Wardrop's first principle. Specifically, based on the latest EV charging price, the following optimization problem can be solved:

$$\boldsymbol{x}_T(k) = \arg\min_{\boldsymbol{x}_T \in \chi_T} F_{MPTA}(\boldsymbol{x}_T, [\boldsymbol{\rho}_a(k-1)]_{a\in\mathcal{E}_{FCS}}) + \text{penalty}_{MPTA}(\boldsymbol{x}_T), \quad (15)$$

where

$$\text{penalty}_{MPTA}(\boldsymbol{x}_T) \triangleq \frac{\gamma}{2}\sum_{t\in\mathcal{T}}\sum_{a\in\mathcal{E}_{FCS}}\left[E_B f_a^t - E_B f_a^t(k-1) + \frac{1}{\gamma}(\rho_a^t(k-1) - \rho_a^t(k-2))\right]^2$$

with $\gamma > 0$ being a control parameter influencing the convergence rate of the MABOST scheme. This term penalizes for failure of convergence, which may be caused by agent misbehavior [24] and result in violation of constraints [9]. It will vanish as the iteration converges, thus will not interfere with the objective of minimizing the operation cost.

Remark 1: In the near future, the task of the traffic agent can be well taken by the fast-growing Internet of Vehicle and Vehicular Cloud (e.g., Google Car), which is a platform collecting data from autonomous vehicles in order to perform a series of tasks [25].

MG-IESP Agent i: The task of this agent is to minimize the operation cost of MG i via energy trading and EV charging service. To achieve this objective, this agent first optimizes its operation schedule $\boldsymbol{x}_i$ based on its current energy selling price and EV charing price, as well as energy selling price bidding from MG agents $\forall j \in \mathcal{N}_i$, which can be formulated as

$$\boldsymbol{x}_i(k) = \arg\min_{\boldsymbol{x}_i\in\chi_i} \text{cost}_{MGi}(\boldsymbol{x}_i, \boldsymbol{\lambda}_i(k-1), [\boldsymbol{\lambda}_j(k-1)]_{j\in\mathcal{N}_i}, [\boldsymbol{\rho}_{y_{FCSij}}(k-1)]_{j\in\mathcal{N}_{FCSi}}) + \text{penalty}_{MGi}(\boldsymbol{x}_i), \quad (16)$$

where

$$\text{penalty}_{MGi}(\boldsymbol{x}_i) \triangleq \frac{\gamma}{2}\sum_{t\in\mathcal{T}}\Bigg\{\sum_{j\in\mathcal{N}_i}\Bigg[P_{i,j}^t - P_{i,j}^t(k-1) + \frac{1}{\gamma}(\lambda_j^t(k-1) - \lambda_j^t(k-2))\Bigg]^2 + \Bigg[P_{outi}^t - P_{outi}^t(k-1) - \frac{1}{\gamma}(\lambda_i^t(k-1) - \lambda_i^t(k-2))\Bigg]^2 + \sum_{j\in\mathcal{N}_{FCSi}}\Bigg[P_{FCSij}^t - P_{FCSij}^t(k-1) - \frac{1}{\gamma}(\rho_{y_{FCSij}}^t(k-1) - \rho_{y_{FCSij}}^t(k-2))\Bigg]^2\Bigg\}$$

is a penalty term functioning similarly as penalty_{MPTA} in (15).

Next, MG-IESP agent i receives the amount of energy its adjacent MGs intend to buy from it (i.e. $\boldsymbol{P}_{i,j}$) and the number of EVs intending to charge at its FCSs (i.e. $\boldsymbol{f}_{y_{FCSij}}$, $j \in \mathcal{N}_{FCSi}$) based on the schedule optimization results of (15) and (16). Then, it regulates its energy selling prices to other MGs and affiliated FCS charging prices according to

$$\rho_{y_{FCSij}}^t(k) = \rho_{y_{FCSij}}^t(k-1) - \frac{\gamma}{2}\overbrace{(P_{FCSij}^t(k) - E_B f_{y_{FCSij}}^t(k))}^{\triangleq r_{FCSij}^t(k)}, \quad (17)$$

$$\lambda_i^t(k) = \lambda_i^t(k-1) - \frac{\gamma}{|\mathcal{N}_i|+1}\underbrace{(P_{outi}^t(k) - \sum_{j\in\mathcal{N}_i}P_{l,i}^t(k))}_{\triangleq r_i^t(k)} \quad (18)$$

Sub-Routine 1: Executed at MG-IESP Agent i

```
Set k = 1: Receive pr_s/pr_b from the main grid agent
while not converged do
  if k = 1 then
    Initialize P_{i,j}(1) = 0 (∀i ∈ N_i), P_outi(1) = 0,
    P_FCSij(1) = 0 (j ∈ N_FCSi)
  else
    Update x_i(k) by optimizing (16)
  end
  Send P_{i,j}(k) to MG-IESP agent j (∀j ∈ N_i)
  Receive P_{j,i}(k) from MG-IEPS agent j (∀j ∈ N_i) and
  f_{y_FCSij} (∀j ∈ N_FCSi) from the traffic agent
  if k = 1 then
    Initialize ρ_{y_FCSij}(0) = ρ_{y_FCSij}(1) = (pr_s + pr_b)/2 · 1
    (∀j ∈ N_FCSi) and λ_i(0) = λ_i(1) = (pr_s + pr_b)/2 · 1
  else
    Update ρ_{y_FCSij}(k) and λ_i(k) following (17) and (18)
  end
  Send ρ_{y_FCSij}(k) to the traffic agent and λ_i(k) to
  MG-IESP agent j ∈ N_i
  Receive λ_j(k) to MG-IESP agent j ∈ N_i
  Set k := k + 1
end
Send P_{0,i}(k) and P_{0,i}(k) to the traffic agent
```

Afterwards, the updated prices $\rho_a^t(k)$ and $\lambda_i^t(k)$ is communicated to the traffic agent and MG-IESP agents $l \in \mathcal{N}_i$, respectively. These price updating rules imitate a price bargaining process in a multi-bilateral trading environment following the classic demand-supply relationship [26]. Specifically, in the energy trading market between a FCS and EVs, P_{FCSij} optimized at MG-IESP agent i is the amount of energy its affiliated FCS intends to supply to EVs at the current charging

price, while $f^t_{y_{FCSij}}$ optimized at the traffic agent denotes the number of EVs to charge at the specific FCS. Similarly, in the energy trading market among adjacent MGs, P_{outi} optimized at MG-IESP agent i can be interpreted as the supply; while $P^t_{l,i}$ optimized at MG-IESP agents can be interpreted as the demand. Based on (17) and (18), if the supply exceeds the demand, the market price λ^t_i (ρ^t_a) should be decreased in the next iteration, and *vice versa*, until the supply and demand finally come to a balance, i.e., the market equilibrium is reached.

Remark 2: It can be observed from (17) and (18) that, when selling energy to the adjacent MGs and EVs, a MG-IESP agent does not adopt a unified price. This actually makes sense as these prices are not only related to the cost of commodity, but are also measures of resource scarcity of charging piles in FCSs, which may differ with respect to locations and EV travel time. In this regard, (17) is designed as a spatial-temporal pricing scheme. Simulation results in Section IV will illustrate that EV charging at a FCS near the city center at busy hour will be charged a higher price, which is in line with our intuition.

Main Grid Agent: The agent can be represented by the transmission system operator. Its objective is to profit from energy trading with the MMGs in a buy-low-sell-high fashion. It does not need to participate in the iterative process with other agents. After the iteration is converged, it just needs to receive information of $\boldsymbol{P}_{i,0}/\boldsymbol{P}_{0,i}$ ($\forall i \in \mathcal{S}_{MG}$) and performs generation scheduling accordingly.

At this point, the detailed procedures of the MABOST scheme can be summarized as Sub-Routines 1 and 2, which can be simultaneously executed at different agents. It can be observed that the information communicated among the agents is all about bidding prices and energy trading quantities, thus the MABOST scheme is a transactive energy based approach and can preserve privacy for each agent. As the centralized formulation (14) is a convex optimization, the MABOST is guaranteed to converge to the optimal solution as it is equivalent to the ADMM in essence [23]. Specifically, MG agent i can locally estimate the maximum 2-norm of the residuals defined in (17) and (18), i.e.,

$$r_{\max,i}(k) = \max\big(|||\boldsymbol{r}_i(k)||_2, \{||\boldsymbol{r}_{FCSij}(k)||_2 | \forall j \in \mathcal{N}_{FCSi}\}\big). \quad (19)$$

If $r_{\max,i}(k)$ is less than a small threshold $\epsilon_{TH} > 0$ (e.g., 10kW in the simulation), it can broadcast a flag to other agents. The MABOST is assumed converged when all the MG agents have sent out their flags.

Sub-Routine 2: Executed at the Traffic Agent

Set $k = 1$
while not *converged* **do**
  if $k = 1$ **then**
    Initialize $\boldsymbol{f}_a(1) = \boldsymbol{0}$ ($\forall a \in \mathcal{E}_T$)
  else
    Update $\boldsymbol{x}_T(k)$ by optimizing (15)
  end
  Send $\boldsymbol{f}_{y_{FCSij}}$ ($j \in \mathcal{N}_{FCSi}$) to MG-IESP agent $i \in \mathcal{S}_{MG}$
  Receive $\boldsymbol{\rho}_{y_{FCSij}}$ from MG-IESP agent $i \in \mathcal{S}_{MG}$
  Set $k := k + 1$
end

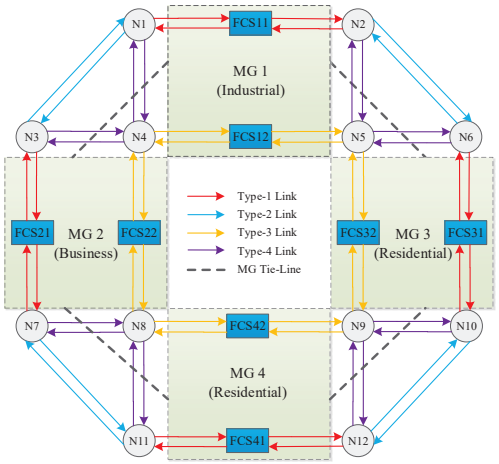

Fig. 2. Interconnection topology of the 4-MG electrical network integrated with FCSs for simulation (All the MGs are connected to the main grid, which is not shown).

IV. Case Study

Numerical analysis is performed in a 4-MG system coupled with a double-ring transportation network, which is depicted in Fig. 2. The topology and basic parameters of the transportation network are from [16]. The parameters relevant to the travel time are shown in Table II. The FCSs at the outer ring are all large, and those at the inner ring are medium except FCS32 being small. The scheduling time horizon is selected as 16:00-20:00 divided into 4 time slots. This period covers the evening peak of urban traffic and is sufficiently long to demonstrate the effectiveness of the MABOST scheme.

TABLE II
Parameters of the Links

Link Type	1	2	3	4	FCS Large	FCS Medium	FCS Small
$c_a/f^{\max}_a$ (p.u.)	100	100	80	60	18	9	6
$t^0_a/t^{\max}_{w,a}$ (min)	5	8	5	7	10	7	3

The vehicle traveling demand is given in Table III, where $tot_{g,rs}$ ($tot_{g,rs}$) denotes the total traveling demand of GVs (EVs) for the specific O-D pair within the time horizon. Consider a distribution factor of each time slot as $\boldsymbol{\beta} = [15\%, 30\%, 35\%, 20\%]$. The scheduled traffic demand of time slot t is $\hat{d}^t_{v,rs} = tot_{v,rs} \times \beta^t$, $v \in \{g, e\}$. The rescheduling cost matrix is selected as $[C]_{t_1 t_2} = \$3|t_1 - t_2|$.

TABLE III
Total Traffic Demand within the Transportation Network

O-D Pair	$tot_{g,rs}$	$tot_{e,rs}$	O-D Pair	$tot_{g,rs}$	$tot_{e,rs}$
N1-N6	120	40	N3-N6	120	40
N1-N10	240	20	N3-N10	200	20
N1-N11	160	40	N3-N11	160	40
N1-N12	160	20	N3-N12	200	20
N4-N9	200	40	N4-N10	160	40
N4-N12	160	40			

In the electrical network, MGs 1-4 serve industrial/business/residential/residential districts, respectively. Only MGs 1 and 2 are equipped with DGs, and the parameters are shown in Table IV. The ordinary load and renewable energy profiles of the MGs are shown in Fig. 3. The main grid energy selling and buyback prices are set as

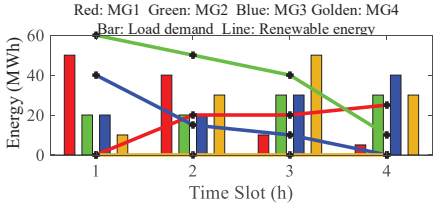

Fig. 3. Load demand and renewable energy of the MGs.

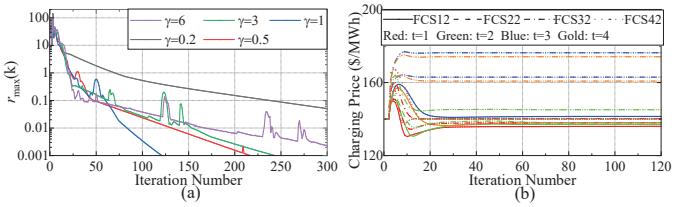

Fig. 4. Iterative process of the MABOST scheme: (a) evolution of the residual at different γ; (b) evolution of the charging prices for FCSs at the inner loop when $\gamma = 1$.

pr_s = \$140/MWh and pr_b = \$80/MWh, and the energy transfer cost between MGs is b_{tran} = \$2/MWh.

TABLE IV
DG PARAMETERS IN MGS 1 AND 2

DG No.	a_{Gi}	b_{Gi}	c_{Gi}	$P_{Gi}^{\min}$	$P_{Gi}^{\max}$
DG 1	\$0.1/(MWh)^2	\$90/MWh	\$0/h	0MWh	250MWh
DG 2	\$0.2/(MWh)^2	\$100/MWh	\$0/h	0MWh	100MWh

A. Simulation Results of the MABOST Scheme

Simulations are implemented using the Matlab-based modeling package CVX [27] to solve the convex optimization subproblem in the agents. The iterative process of the MABOST scheme is plotted in Fig. 4. Fig. 4(a) shows the evolution of the maximum residual at different γ, which is defined as

$$r_{\max}(k) = \max\left(r_{\max,1}(k), \cdots, r_{\max,|\mathcal{S}_{MG}|}(k)\right). \quad (20)$$

Observe that when γ is too low or high, the convergence will be significantly delayed. When $\gamma = 1$, the scheme can converge quickly within 62 iterations. Fig. 4(b) shows evolution of the charging prices for FCSs at the inner loop when $\gamma = 1$. Considering that parallel computing can be further implemented, the converging performance is satisfactory.

Fig. 5 plots energy trading and scheduling of the MGs after the MABOST iteration converges. As MG 1 possesses a bulk DG with relatively cheap generation cost, it always plays the role of an energy producer for its adjacent MGs. Specifically, in the first 2 hours, as MG 2 has a high level of renewable output, it is almost self-sufficient and only needs to import a small amount of energy. Similarly, as the net load level of MG 3 and its EV charging load is also low, it only needs to purchase cheap energy from MG 1 rather than the main grid. Moreover, MG 4 can indirectly (i.e., via two hops) purchase energy from MG 1 at $t = 1$ as it is still cheaper than pr_s. In the last 2 hours, as the ordinary and EV charging loads increase while the renewable energies decrease, MGs 2 and 3 import more energy from MG 1 until λ_1^t reaches \$138/MWh. Above these level, they would rather purchase energy from the main grid. Thus, their energy selling prices become \$140/MWh.

Regarding the transportation network, we first test the influence of flexible demand on traffic distribution. Fig. 6 plots the east-bound traffic flows (including both GVs and EVs) in MG 1 considering both fixed and flexible demand. The night

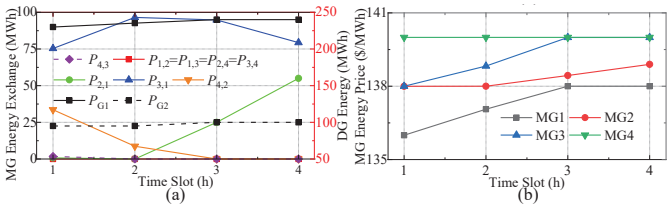

Fig. 5. Energy trading and scheduling of the MGs: (a) MG energy generation and exchange; (b) MG energy trading prices.

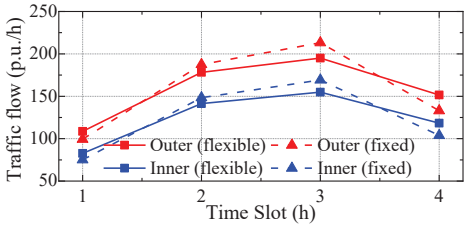

Fig. 6. East-bound traffic flows of the inner- and outer-ring road in MG 1.

peak (17:00-19:00) traffic is obviously shaved by rescheduling the vehicles to less busy time slots. Moreover, there exists more traffic in the outer ring than the inner ring because the roads have larger capacities and the FCS has more charging space. Traffic in the other roads of the two rings exhibit similar phenomenon, but are not shown in the paper.

Then, influence of the spatial-temporal based flexible pricing for EV charing is investigated. It can be observed from Fig. 7(a) the prices of each FCS in the first 2 hours are generally cheaper than the last 2 hours. This is because the renewable energies of the MGs are generally high while the traffic demands are relatively low in the first 2 hours. Fig. 7(b) shows that most of the FCSs in the outer loop still have space to service EVs except FCS21. An in-depth study reveals that this is because FCS21 locates on the routes of many O-D pairs. If EVs choose other routes passing less crowded FCSs, their travel time would be significantly higher. In comparison, FCS12, FCS22 and FCS32 in the inner loop are saturated in the traffic peak (i.e., $t = 3$) due to the limited waiting areas and high travel demands, which leads to price premiums for EV charging in these locations (as can be seen in Fig. 7(a)). FCS42 always remains unsaturated because less routes visit it. FCS32 is the only small FCS in the transportation network, and thus its charging prices at all time slots are the highest because of resource scarcity.

B. Comparison with a Base Case

This subsection compares the simulation results with those of a base case to demonstrate effectiveness of the MABOST scheme. The base case prohibits energy trading among the MGs and adopts a unified and time-invariant EV charging price equal to pr_s for all the FCSs. Flexibility of EV traveling

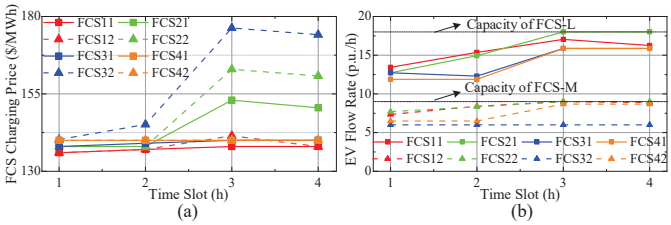

Fig. 7. Operation of the FCSs: (a) Charging prices and (b) EV flow rates at the FCSs.

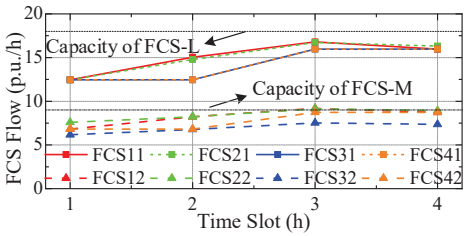

Fig. 8. EV flow rates entering the FCSs in the base case.

time is still considered as it characterizes drivers' intrinsic behavior regardless of the scheduling method. In this situation, the EV flows entering the FCS for charging are plotted in Fig. 8. It indicates that the flow rates of FCSs in the inner ring except FCS42 exceed $f_a^{\max}$ at $t = 3$. Specifically, due to the extremely limited charging piles, flow rates of FCS32 in all time slots exceed $f_a^{\max}$, which can lead to a high probability that the upcoming EVs cannot be serviced and deteriorate the social welfare.

Next, we compare the revenue of each MG (i.e., $-\text{cost}_{MGi}$) under the MABOST scheme and the base case. The results are shown in Table V, which indicate that the MMGs can achieve a satisfactory revenue increase of 13.5% as a whole, but the increase rate of each MG differs a lot. The revenues mainly come from two sources, i.e., selling cheap energy to adjacent MGs and price premium from EV charging. Specifically, MGs 1 and 2 have large scales of cheap DG capacity and renewable energy, thus they mainly profit from the former source, as indicated by Fig. 5. On the other hand, MG 3 mainly profit from the later source because of the scarcity of charging resource, e.g., in an old residential district with limited space to construct FCSs. The MABOST scheme can only trivially increase the revenue of MG 4. This is reasonable because MG 4 has no generation capacity and the selling prices of adjacent MGs are no less than the main grid retail price considering the energy transfer cost. Moreover, there is no EV charging premium in this area because there is less traffic and plenty of charging resource, e.g., in a new residential district.

TABLE V
COMPARISON OF MG REVENUES

Case \ Revenue/$	MG1	MG2	MG3	MG4	Total
Base	27870	30039	10100	0	68009
MABOST	31799	33948	11427	0.15	77174
Increase Rate	14.0%	13.1%	11.3%	n/a	13.5%

V. CONCLUSIONS

The promotion of electric vehicles (EVs) strengthens the coupling between the electrical and transportation systems, and necessitates to co-optimize them simultaneously. To this end, this paper has proposed a multi-agent based optimal scheduling and trading (MABOST) scheme for multiple microgrids (MGs) integrated fast charging stations (FCSs). Within the scheme, a multi-period convex optimization algorithm has been designed to calculate the traffic flow distributions in the user equilibrium assuming the electric/gasoline vehicle drivers all act rationally to minimize its own travel expense and are flexible to reschedule their travel time at a certain cost of inconvenience. The MGs have been modeled to make profit from trading superfluous energy with adjacent MGs and providing EV charging service with its FCSs. The transactive energy based MABOST scheme guides each agent to act rationally for the sake of its own benefit. This process imitates price negotiation in a multi-bilateral energy trading environment, and is guaranteed to converge to an market equilibrium. Simulation results of a electrical network consisting of 4 MGs coupled with a double-ring transportation network have demonstrated that the proposed scheme can not only increase the revenue of each MG, but also improve the traffic condition by alleviating rush-hour traffic and overcrowding of FCSs in the city center.

APPENDIX A
JUSTIFICATION OF FCS FLOW-TIME FUNCTION (6)

Compared to the FCS flow-time function in [16] based on the *M/M/1* model [20], it is more appropriate to adopt the *M/M/c/K* model, where c and K stand for the number of charging poles and the maximum number of EVs allowed to stay in the FCS, respectively. Generally, $K \geq c$, but it is not unlimited, especially for FCSs in metropolitan cities. In this regard, it is possible that a forthcoming EV cannot be serviced. This corresponds to a lost probability which is influenced by K.

Based on the queuing theory [19], the probability P_i that a total number of i EVs stay in the FCS can be calculated as

$$P_0 = \left(\sum_{n=0}^{c-1} \frac{(f_a^t)^n}{n!\mu^n} + \sum_{n=c}^{K} \frac{(f_a^t)^n}{c^{n-c}c!\mu^n} \right)^{-1}, \tag{21}$$

$$P_n = \begin{cases} \dfrac{(f_a^t)^n}{n!\mu^n} P_0 & 0 \leq n \leq c \\ \dfrac{(f_a^t)^n}{c^{n-c}c!\mu^n} P_0 & c \leq n \leq K \end{cases}. \tag{22}$$

Specifically, the lost probability is equivalent to P_K. The average time an EV spending in the FCS can be calculated as

$$t_a(f_a^t) = \frac{1}{\mu} + \frac{\sum_{n=c+1}^{K}(n-c)P_n}{(1-P_K)f_a^t}, \tag{23}$$

where the first and second terms account for charging and queuing time, respectively.

Consider that the expressions for $t_a(f_a^t)$ are too complicated to be used for optimization, it is preferred to approximate it with a simplified function. Specifically, consider that $c = 4$p.u., $\mu = 3$p.u., the average service time t_a and lost probability P_K with different number K under different EV flow rate f_a^t are plotted in Fig. 9. Fig. 9(b) indicates that the lost probability is proportional to f_a^t and is inversely proportional to K. It also shows that to restrict the lost probability within a certain limit (e.g., 10%), f_a^t should be upper bounded by a corresponding $f_a^{\max}$. Fig. 9(a) shows that whe $f_a^t \leq f_a^{\max}$ (i.e., the part of curves to the left of the '+' sign) under different K, the cubic function (6) is sufficiently accurate to approximate the actual waiting time.

APPENDIX B
PROOF OF PROPOSITION 1

Incorporating the definitional constraints (2) and (4) as functions of the decision vector, i.e., $D_{v,rs}(\boldsymbol{x}_T)$ $(v \in \{g, e\})$

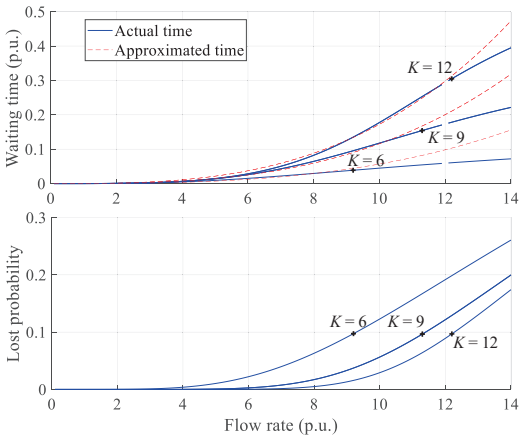

Fig. 9. Approximation of the FCS flow-time function: (a) actual and approximated times and (b) probability rate under different flow rate ('+' sign corresponds to a tolerant lost probability of 10%).

and $\boldsymbol{f}_a(\boldsymbol{x}_T)$, the Lagrange function of (12) with respect of the equality constraint (1) and inequality constraint (3) can be formulated as

$$\begin{aligned} &L_{MPTA}(\boldsymbol{x}_T, \boldsymbol{\mu}_T) = \\ &\sum_{t_i\in\mathcal{T}}\Bigg[\omega\sum_{a\in\mathcal{E}_T}\int_0^{f_a^{t_i}(\boldsymbol{x}_T)} t_a(\xi)d\xi + \sum_{a\in\mathcal{E}_{FCS}}\rho_a^{t_i}E_B f_a^{t_i}(\boldsymbol{x}_T) \\ &\quad + \sum_{t_j\in\mathcal{T}}\sum_{v\in\{g,e\}}\sum_{(m,n)\in\mathcal{D}_T}[C]_{t_it_j}[D_{v,mn}(\boldsymbol{x}_T)]_{t_it_j}\Bigg] \\ &\quad + \sum_{v\in\{g,e\}}\sum_{(m,n)\in\mathcal{D}_T}\Bigg\{\boldsymbol{\mu}_{v,mn}^{\intercal}\left[\hat{\boldsymbol{d}}_{v,mn} - D_{v,mn}(\boldsymbol{x}_T)\mathbf{1}\right] \\ &\qquad - \sum_{h=1}^{N_{v,mn}}\sum_{t_i,t_j\in\mathcal{T}}\nu_{v,mn,h}^{t_it_j}\left[F_{v,mn,h}\right]_{t_it_j}\Bigg\} \end{aligned} \tag{24}$$

where $\boldsymbol{\mu}_T \triangleq \{\boldsymbol{\mu}_{v,mn}|\forall v = \{g,e\},(m,n) \in \mathcal{D}_T\}$ and $\boldsymbol{\nu}_T \triangleq \{\nu_{v,mn,h}^{t_it_j}|\forall v = \{g,e\},(m,n) \in \mathcal{D}_T, h \in \{1,\cdots,N_{v,mn}\}, t_i, t_j \in \mathcal{T}\} \geq \mathbf{0}$ are the vectors of Lagrangian multipliers.

Further considering that

$$\frac{\partial f_a^{t_i}(\boldsymbol{x}_T)}{\partial[F_{v,rs,h}]_{t_1t_2}} = \begin{cases} 0 & t_i \neq t_2 \\ [\Delta_{g,rs}]_{ah} & t_i = t_2, v = g \\ [\Delta_{e,rs}]_{ah} & t_i = t_2, v = e \end{cases},$$

$$\frac{\partial[D_{v_1,mn}(\boldsymbol{x}_T)]_{t_it_j}}{\partial[F_{v_2,rs,h}]_{t_1t_2}} = \begin{cases} 1 & v_1 = v_2, mn = rs, t_it_j = t_1t_2 \\ 0 & \text{otherwise} \end{cases},$$

the optimal solution of (12) satisfies the Karush-Kuhn-Tucker conditions as follows:

Stationarity

$$\begin{aligned} \frac{\partial L_{MPTA}}{\partial[F_{g,rs,h}]_{t_1t_2}} &= \omega\sum_{a\in\mathcal{E}_T}[\Delta_{g,rs}]_{ah}f_a^{t_2} + [C]_{t_1t_2} - \mu_{g,rs}^{t_1} - \nu_{g,rs,h}^{t_1t_2} \\ &= \text{cost}_{g,rs,h}^{t_1t_2} - \mu_{g,rs}^{t_1} - \nu_{g,rs,h}^{t_1t_2} = 0 \end{aligned} \tag{25a}$$

$$\begin{aligned} &\frac{\partial L_{MPTA}}{\partial[F_{e,rs,h}]_{t_1t_2}} = \omega\sum_{a\in\mathcal{E}_T}[\Delta_{e,rs}]_{ah}f_a^{t_2} + \rho_{y_{e,rs,h}}^{t_2}E_B + [C]_{t_1t_2} \\ &- \mu_{e,rs}^{t_1} - \nu_{e,rs,h}^{t_1t_2} = \text{cost}_{e,rs,h}^{t_1t_2} - \mu_{e,rs}^{t_1} - \nu_{e,rs,h}^{t_1t_2} = 0 \end{aligned} \tag{25b}$$

Complementary slackness

$$\nu_{v,rs,h}^{t_1t_2}\left[F_{v,rs,h}\right]_{t_1t_2} = 0 \tag{25c}$$

It follows from (25a) and (25b) that

$$\nu_{g,rs,h}^{t_1t_2} = \text{cost}_{g,rs,h}^{t_1t_2} - \mu_{g,rs}^{t_1} \geq 0, \tag{26a}$$

$$\nu_{e,rs,h}^{t_1t_2} = \text{cost}_{e,rs,h}^{t_1t_2} - \mu_{e,rs}^{t_1} \geq 0. \tag{26b}$$

Substituting (26a) and (26b) into (25c) leads to (11), which completes the proof of the proposition.

REFERENCES

[1] S. A. Arefifar, Y. A.-R. I. Mohamed, and T. El-Fouly, "Optimized multiple microgrid-based clustering of active distribution systems considering communication and control requirements," *IEEE Trans. Ind. Electron.*, vol. 62, no. 2, pp. 711–723, Feb. 2015.

[2] Y. Liu, Y. Li, H. B. Gooi, Y. Jian, H. Xin, X. Jiang, and J. Pan, "Distributed robust energy management of a multimicrogrid system in the real-time energy market," *IEEE Trans. Sustain. Energy*, vol. 10, no. 1, pp. 396–406, 2019.

[3] A. Paudel, K. Chaudhari, C. Long, and H. B. Gooi, "Peer-to-peer energy trading in a prosumer-based community microgrid: A game-theoretic model," *IEEE Trans. Ind. Electron.*, vol. 66, no. 8, pp. 6087–6097, 2018.

[4] Y. Li, T. Zhao, P. Wang, H. B. Gooi, L. Wu, Y. Liu, and J. Ye, "Optimal operation of multimicrogrids via cooperative energy and reserve scheduling," *IEEE Trans. Ind. Informat.*, vol. 14, no. 8, pp. 3459–3468, 2018.

[5] M. D. Ilic, "From hierarchical to open access electric power systems," *Proc. IEEE*, vol. 95, no. 5, pp. 1060–1084, May 2007.

[6] D. Gregoratti and J. Matamoros, "Distributed energy trading: the multiple-microgrid case," *IEEE Trans. Ind. Electron.*, vol. 62, no. 4, pp. 2551–2559, Apr. 2015.

[7] H. Wang and J. Huang, "Incentivizing energy trading for interconnected microgrids," *IEEE Trans. Smart Grid*, vol. 9, no. 4, pp. 2647 – 2657, Jul. 2018.

[8] M. Marzband, N. Parhizi, M. Savaghebi, and J. M. Guerrero, "Distributed smart decision-making for a multi-microgrid system based on a hierarchical interactive architecture," *IEEE Trans. Energy Convers.*, vol. 31, no. 2, pp. 637–648, Apr. 2016.

[9] W.-J. Ma, J. Wang, V. Gupta, and C. Chen, "Distributed energy management of networked microgrids using online ADMM with regret," *IEEE Trans. Smart Grid*, vol. 9, no. 2, pp. 847–856, 2018.

[10] E. L. Karfopoulos, P. Papadopoulos, S. Skarvelis-Kazakos, I. Grau, L. M. Cipcigan, N. Hatziargyriou, and N. Jenkins, "Introducing electric vehicles in the microgrids concept," in *Int. Conf. Intell. Syst. Appl. Power Syst.*, Hersonissos, Greece, Sep. 2011, pp. 1–6.

[11] D. Wang, X. Guan, J. Wu, P. Li, P. Zan, and H. Xu, "Integrated energy exchange scheduling for multimicrogrid system with electric vehicles," *IEEE Trans. Smart Grid*, vol. 7, no. 4, pp. 1762–1774, 2016.

[12] S. Zou, Z. Ma, and N. Yang, "Decentralised hierarchical coordination of electric vehicles in multi-microgrid systems," *IET Gen. Transm. Distrib.*, vol. 13, no. 13, pp. 2899–2906, 2019.

[13] H. Engel, R. Hensley, S. Knupfer, and S. Sahdev. (2018, Aug.) Charging ahead: Electric-vehicle infrastructure demand. [Online]. Available: https://www.mckinsey.com/industries/automotive-and-assembly/our-insights/charging-ahead-electric-vehicle-infrastructure-demand

[14] W. Wei, S. Mei, L. Wu, J. Wang, and Y. Fang, "Robust operation of distribution networks coupled with urban transportation infrastructures," *IEEE Transactions on Power Systems*, vol. 32, no. 3, pp. 2118–2130, 2017.

[15] M. Alizadeh, H.-T. Wai, M. Chowdhury, A. Goldsmith, A. Scaglione, and T. Javidi, "Optimal pricing to manage electric vehicles in coupled power and transportation networks," *IEEE Trans. Control Netw. Syst.*, vol. 4, no. 4, pp. 863–875, 2016.

[16] W. Wei, L. Wu, J. Wang, and S. Mei, "Network equilibrium of coupled transportation and power distribution systems," *IEEE Trans. Smart Grid*, vol. 9, no. 6, pp. 6764–6779, 2018.

[17] H. K. Nunna and D. Srinivasan, "Multiagent-based transactive energy framework for distribution systems with smart microgrids," *IEEE Trans. Ind. Informat.*, vol. 13, no. 5, pp. 2241–2250, 2017.

[18] A. E. Ohazulike, G. Still, W. Kern, and E. C. van Berkum, "An origin–destination based road pricing model for static and multi-period traffic assignment problems," *Transp. Res. Part E Log. Transp. Rev.*, vol. 58, pp. 1–27, 2013.
[19] J. Sztrik, "Basic queueing theory," *Debrecen, Hungary: Univ. Debrecen,*, vol. 193, pp. 60–67, 2012.
[20] R. Akçelik, "Travel time functions for transport planning purposes: Davidson's function, its time dependent form and alternative travel time function," *Aust. Road Res.*, vol. 21, no. 3, pp. 49–59, 1991.
[21] J. G. Wardrop, "Road paper. some theoretical aspects of road traffic research." *Proc. Inst. Civ. Eng.*, vol. 1, no. 3, pp. 325–362, 1952.
[22] Y. Sheffi, *Urban transportation networks: Equilibrium Analysis With Mathematical Programming Methods*, 1st ed. Englewood Cliffs, NJ: Prentice-Hall, 1985.
[23] S. Boyd, N. Parikh, E. Chu *et al.*, "Distributed optimization and statistical learning via the alternating direction method of multipliers," *Found. Trends Mach. Learn.*, vol. 3, no. 1, pp. 1–122, Jan. 2011.
[24] Y. Liu, H. B. Gooi, Y. Li, H. Xin, and J. Ye, "A secure distributed transactive energy management scheme for multiple interconnected microgrids considering misbehaviors," *IEEE Trans. Smart Grid*, vol. 10, no. 6, pp. 5975–5986, 2019.
[25] E.-K. Lee, M. Gerla, G. Pau, U. Lee, and J.-H. Lim, "Internet of vehicles: From intelligent grid to autonomous cars and vehicular fogs," *Int. J. Distrib. Sensor Netw*, vol. 12, no. 9, pp. 1–14, 2016.
[26] D. Gan, D. Feng, and J. Xie, *Electricity Markets and Power System Economics*, 1st ed. Boca Raton, FL: CRC Press, 2013.
[27] M. Grant, S. Boyd, and Y. Ye. (Oct. 2016) CVX: Matlab software for disciplined convex programming. [Online]. Available: http://cvxr.com/cvx/.